ISSN 1392-1207. MECHANIKA. Vol. 29, No. 6, 2023: 530–538

An ON-OFF Closed-Loop Control of Photoelectric Actuator Based on PLZT Ceramic

Yafeng LIU*, Yiwei YANG, Chunbo LIU***, Xinjie WANG******
**School of Electromechanical Engineering, Henan University of Technology, Zhengzhou 450001, China*
E-mail: yfliu@haut.edu.cn (Corresponding author)
***School of Electromechanical Engineering, Henan University of Technology, Zhengzhou 450001, China*
****School of Electromechanical Engineering, Henan University of Technology, Zhengzhou 450001, China*
*****School of Mechanical Engineering, Nanjing University of Science and Technology, Nanjing 210094, China*
https://doi.org/10.5755/j02.mech.33716

1. introduction

In today's era of rapid development of high-tech industry, the technology of precision drive field has been brought to a higher level by the new driving methods based on smart materials. Among them, the photovoltaic smart material, PLZT ceramic with its photostrictive effect has shown its excellent performance in practical applications. Specifically, PLZT ceramic irradiated by ultraviolet light can convert light energy into electrical energy, which generates photoelectric fields. Therefore, PLZT ceramic can be used as optical drive source of electrostatic actuator and other driving systems. Thus, it has the advantages of no external excitation electromagnetic source, favourable independency, non-contact control and clean energy [1]. Moreover, according to the photostrictive effect, PLZT ceramic is not only widely used in optical modulators, sensors and holographic memory, but also has broad application prospects in vibration and active control fields.

Over the past years, scholars have investigated in-depth studies focusing on the practical application of PLZT ceramic in microdrive area. Yue et al. [2] proposed a PLZT/PVDF hybrid drive contactless shape adjustment method and proved its effectiveness in cantilever beam deformation control. The high-performance transparent PLZT ceramic fiber made by Chen [3] can be used to manufacture high-frequency ultrasonic transducers and apply in the field of imaging. The transverse deflection of PLZT optical actuator under different conditions is studied by Mosfequr and Mahbub [4]. Based on the model of 0-3 polarized PLZT ceramic, Wang et al. [5] deduced the nonlinear algebraic equation through simplification and finally used to characterize the size effect field. Chen et al. [6] established the constituent equations of PLZT micro-cantilevers and discussed the size dependence of PLZT microcantilever beam after polarization. Meanwhile A microgripper for biomedical applications was designed by Luis [7] with a rotating electrostatic comb actuator. Batra and Kotru [8] used SETFOS for the first time to simulate photovoltaic devices based on PLZT thin films to study the performance of photovoltaic devices. Several factors affecting the optimum dust removal design of comb electrodes were explored by Jiang et al. [9]. The results improved the dust removal efficiency of the system. Jiang and Huang [10] proposed a PZT electrostatic exclusion drive mechanism which can be remotely controlled to meet the control accuracy requirements.

Meanwhile, PLZT ceramic also show great application potential in vibration, active control and other fields. Irschik H. et al. [11] solved the vibration problem by studying piezoelectric actuation of beam structure and solving dynamic shape control. Shih H. R. et al. [12] investigated the active vibration control behavior of the photostrictive opto-electromechanical actuators and the control of shell components. An optical tracking device based on transparent PLZT material was designed and analyzed by Mahmoud pour M. et al. [13] to find the reasonable value of lateral deflection. An optical driven servo system with improved on–off control strategy were proposed by Lu et al. [14] to decrease the undesirable fluctuation around the target displacement based on PLZT ceramic. The SOFSMC method was used by He et al. [15] to reduce the multimodal vibration of the new photoelectric laminated cylindrical shell with the multi-chip actuating structure as well as the inherent flutter of the conventional control. Jiang et al. [16] designed a logical switch between the PLZT generator and the piezoelectric actuator to acquire the initial voltage of the piezoelectric actuator. PLZT ceramic was made as actuators by Gou X. and Liu B. [17] and the proposed fuzzy neural network controller can effectively control the vibration of intelligent laminated simply supported plates. Bakhtiari I. et al. [18] first investigated the nonlinear forced vibration analysis of thin curved beams with optical actuators. A piezoelectric actuator that can realize bidirectional displacement amplification is proposed by Huang [19] and used to reduce nonlinear errors.

In our previous work [20], the driving characteristics and influence factors of novel photoelectric actuator based on PLZT ceramic were studied. However, due to the lack of investigation on the servo system of photoelectric actuator based on PLZT ceramic in the relevant literature, it is urgent to further study the control characteristics of the photoelectric actuator based on PLZT ceramic. Therefore, in this article, a new closed-loop control method with ON-OFF control strategy is proposed, and the closed-loop control mechanism is described. Taking the driving voltage and output displacement of photoelectric actuator as the control objects, then control equations of the driving voltage and output displacement are built, and the control effect is studied by a variety of experiments and numerical simulation analysis. The closed-loop control research can be applied to many fields such as micro mirrors in the future to improve the dynamic precision control of actuators.

2. Mathematical model of the photoelectric actuator

Based on our previous work [20], the schematic diagram of the photoelectric actuator is illustrated in Fig. 1.

Its working principle is that when PLZT ceramic is illuminated by UV light source, according to photostrictive effect, the photoinduced carriers are generated inside the material, then a high photoinduced voltage is generated and then applied to the driven load by wires, finally the electrostatic field is engendered between the two electrodes. At this point, the upper electrode is rotated downward to a certain angle under the action of electrostatic force, so as to have the output displacement. When the light source stops illuminating, the upper electrode of the driven load restores to the initial position driven by the torsion arm. Therefore, it is possible to control the driving voltage and output displacement by applying light to the PLZT ceramic for opto-electrostatic hybrid torsion driving.

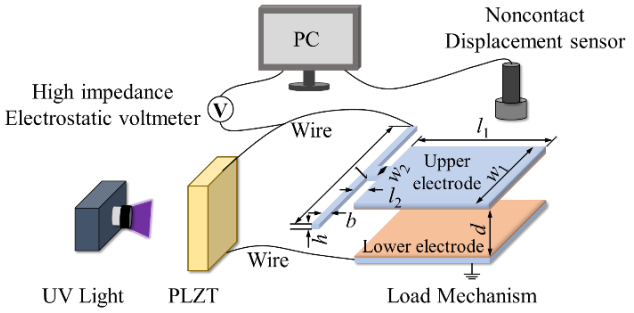

Fig. 1 Schematic diagram of the photoelectric actuator

The torsion beam structure is used in driven load and its displacement diagram is shown in Fig. 2, θ represents the torsion angle of the photoelectric actuator. The size parameters of the photoelectric actuator can be shown in Table 1. The main material of the torsion beam structure is PMMA (Polymethyl Methacrylate). Two conductive copper foils are applied with insulating adhesive to the lower and upper surfaces of the upper electrode and the lower electrode, which is shown in Fig. 3.

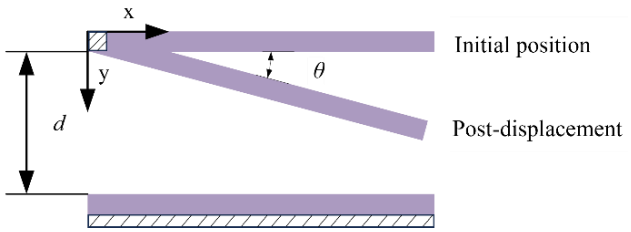

Fig. 2 Displacement diagram of load mechanism

Table 1

The parameters and values of the actuator

Parameters	l	l_1	l_2	ω_1	ω_2	b	h	d
Values, mm	28.5	40	0.3	20	2	2	1	4

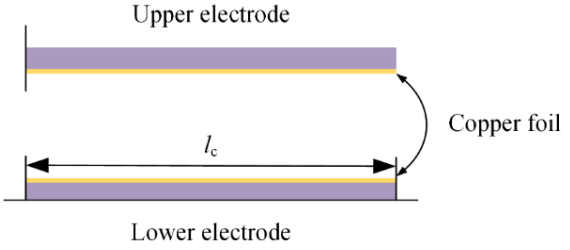

Fig. 3 Component diagram of load mechanism

Based on our previous work, the following mathematical relationships of photovoltage, torsion angle θ and output displacement S can be obtained when the driving structure is in equilibrium:

$$\left.\begin{aligned} U^2 &= \frac{4\theta^3 Gbh^3\left[1-\frac{192h}{b\pi^5}tanh\left(\frac{\pi b}{2h}\right)\right]}{3\varepsilon_0\omega_1 l\left(\ln\frac{d-l_1\theta}{d}+\frac{l_1\theta}{d-l_1\theta}\right)} \\ S &= l_1\theta \end{aligned}\right\}, \tag{1}$$

where: ε_0 and G are the permittivity of vacuum and modulus of elasticity.

In this paper, for the photoelectric actuator, the load mechanism is equivalent to a parallel plate capacitance structure. Therefore, when the two parallel electrodes of the driven load and PLZT ceramic are connected, it equals to the resistance R_1 and capacitor C_1 connected in parallel to the PLZT ceramic. Therefore, as shown in Fig. 4, the load mechanism is in parallel with PLZT ceramic, I_p is the photocurrent produced by PLZT ceramic under ultraviolet light, and U is the driving voltage of photoelectric actuator.

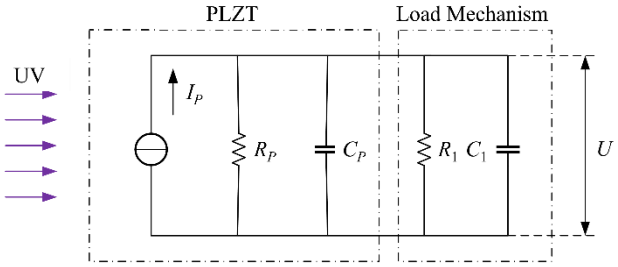

Fig. 4 Equivalent electrical model of photoelectric actuator

On the basis of the driving equivalent electrical model in Fig. 4, the equations of total capacitance and resistance can be expressed:

$$\left.\begin{aligned} C &= C_p + C_1 \\ R &= \frac{R_p \cdot R_1}{R_p + R_1} \end{aligned}\right\}. \tag{2}$$

Then the driving voltage is:

$$U = I_p \frac{R_p \cdot R_1}{R_p + R_1}\left(1-e^{-t/\tau'}\right) = U_s'\left(1-e^{-t/\tau'}\right), \tag{3}$$

where: τ' is the new time constant, its equation is:

$$\tau' = \frac{R_p \cdot R_1}{R_p + R_1}\left(C_p + C_1\right). \tag{4}$$

3. Closed-loop control mechanism of photoelectric actuator

Previous experimental works on the performance of the photoelectric actuator have shown that the proposed driving method has superior output displacement characteristics, and the magnitude of the driving voltage directly affects the output displacement, which determines the driving performance. Therefore, the output displacement remains the same when the driving source and load size remain unchanged and the driving voltage is fixed; when the driving

voltage changes to another constant value, the output displacement changes to another constant value. In addition, the output displacement data of the photoelectric actuator can be measured, collected and fed back to the computer, and the control command can be sent by comparing the output displacement value with the target displacement value in real time. Therefore, driving voltage or output displacement can be used as control variables to realize effective closed-loop control by determining the appropriate control strategy. Figs. 5 and 6 show that the schematic and block diagrams of active control for the photoelectric actuator.

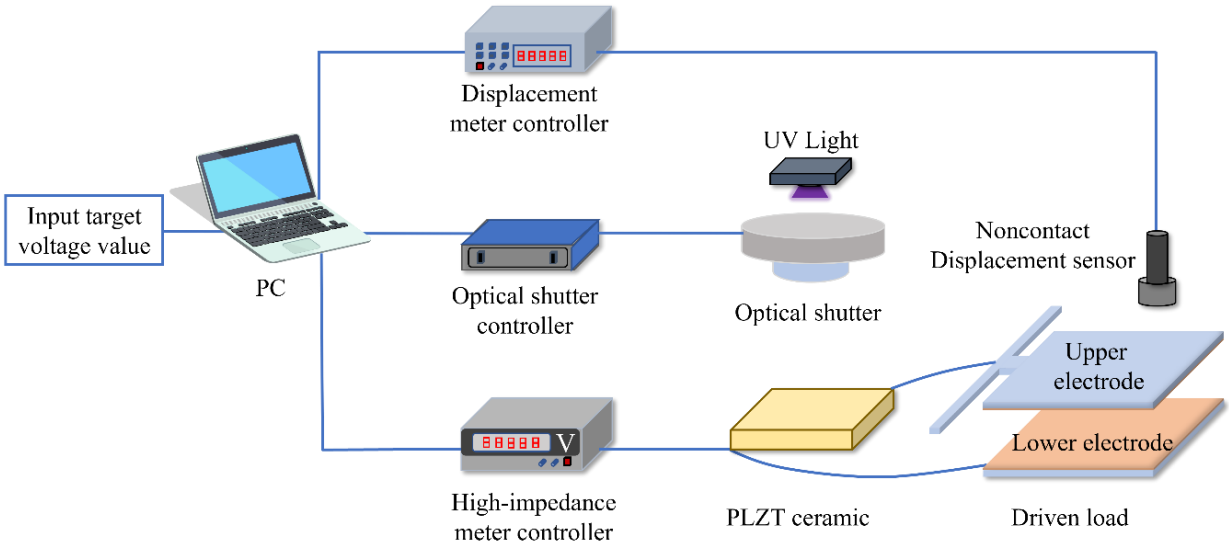

Fig. 5 Schematic diagram of active control for the photoelectric actuator

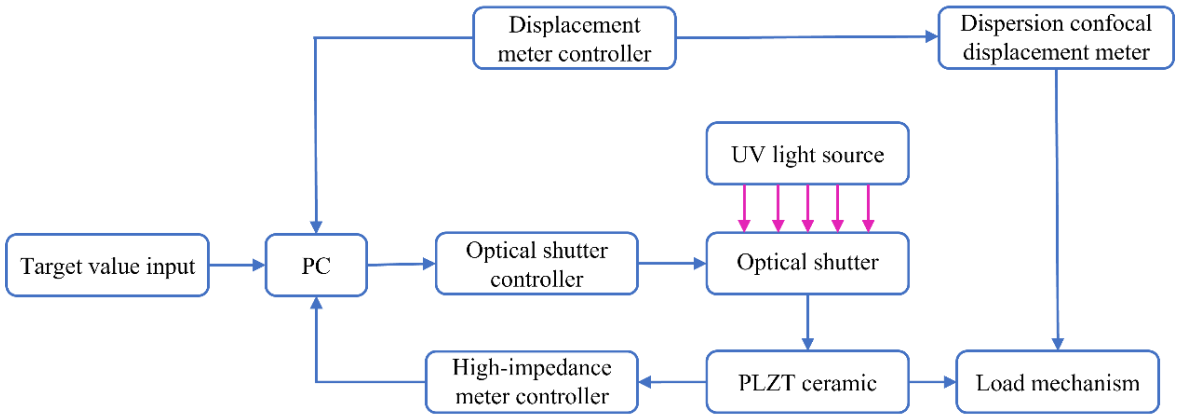

Fig. 6 Block diagram of active control for the photoelectric actuator

As can be seen from the above schematic and block diagram in Figs. 5 and 6, the values of driving voltage and output displacement are detected in real time, and the data can be collected and transmitted to the computer. When the output displacement is to meet a specific target value in a certain working environment, the driving voltage or the output displacement needs to be stable and fluctuate around a certain value. Therefore, the ON-OFF of light source can be controlled by controlling the optical shutter state. When the driving voltage or output displacement is greater than a specific value, the optical shutter is closed. When the driving voltage or output displacement is less than a certain value, the optical shutter is opened, so that the dynamic closed-loop control of the actuator can be achieved.

Thus, the specific control principle is: the input of the target value (voltage value U_g or displacement value S_g) is set at the computer terminal, the driving voltage U and output displacement S of the photoelectric actuator are monitored in real time by the high-impedance electrostatic voltmeter and the high resolution confocal chromatic sensor. By comparing the magnitudes between U_g and U, S_g and S, ON-OFF control of the UV light source is performed. When the driving voltage U or the output displacement S is less than or equal to the target voltage value U_g or the displacement value S_g, the optical shutter is opened, and the PLZT ceramic is illuminated, so the driving voltage and the output displacement of the actuator increase. While when the driving voltage U or the output displacement S is greater than the target voltage value U_g or the displacement value S_g, the optical shutter is closed, and the PLZT ceramic is no longer illuminated, at this time, the driving voltage of the actuator decreases, and the output displacement also decreases. The effect of active control can be observed through the displacement data fed back to the computer by the high resolution confocal chromatic sensor. The simulation ends when the simulation time t reaches the set total time t_g. Fig. 7 shows the schematic diagram of the entire algorithm flow during the control period.

As shown in Fig. 7, in the whole control process, the driving voltage U or output displacement S of the actuator should be constantly approached the target voltage value

U_g or displacement value S_g. Therefore, in the implementation of the ON-OFF control strategy, the process of judging and controlling the optical shutter shown in Fig. 7 should be repeated continuously until the total simulation time t_g ends.

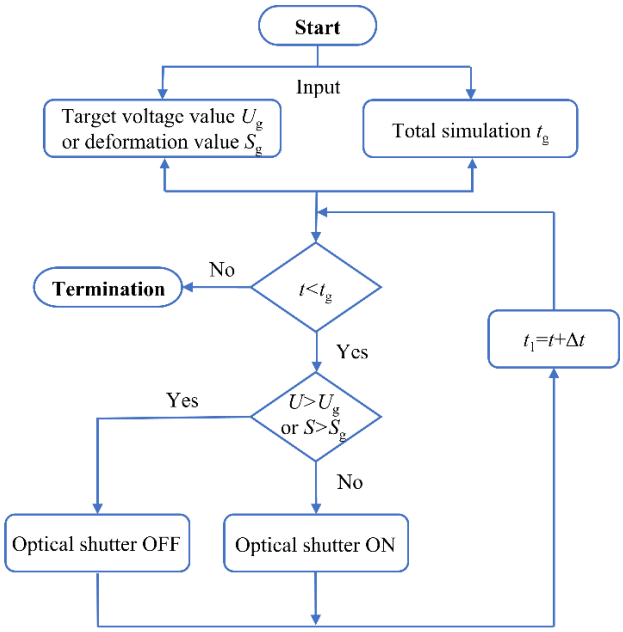

Fig. 7 Diagram of ON-OFF control strategy flow

4. Closed-loop control of driving voltage

4.1. Closed-loop control model of driving voltage

Because the control process involves the optical shutter on and off, that is to control the light source irradiation and closure. Therefore, it is necessary to establish the expressions of driving voltage in the light on and light off phases. According to relevant literature, the equation of photovoltage in light off phase is:

$$U_f(t) = U_0 + k_f e^{-\frac{t}{\tau_f}}, \tag{5}$$

where: U_0 is the initial voltage; k_f is the variation coefficient of residual voltage, which is determined by the thermal parameters and residual polarization intensity of PLZT ceramic. τ_f is the dark time constant.

On the basis of the expression of the driving voltage in the light-on phase in the Eq. (3), the expressions of the driving voltage in the light on and light off phases can be acquired simultaneously with the Eq. (5):

$$\left.\begin{aligned} U(t) &= U_s'(1-e^{-\frac{t}{\tau}}) \\ U_f(t) &= U_0 + k_f e^{-\frac{t}{\tau_f}} \end{aligned}\right\}. \tag{6}$$

For a given cycle time T, a complete ON-OFF control will go through the following steps:

1. The driving voltage value U_i is obtained by the high-impedance voltmeter obtains at a certain time, the computer terminal judges the ON/OFF state of the optical shutter through the control strategy, and the target voltage value U_g is input on the computer;

2. If the optical shutter is opened, the PLZT ceramic is in the illumination phase, and the driving voltage value of the high-impedance voltmeter in the next sampling period can be calculated by Eq. (7):

$$\left.\begin{aligned} U &= U_i + U^{-1}(U_f(t_{n_j}))\Delta t && (a) \\ t_{n_j} &= U_f^{-1}(U(t_{m_j})) \quad (U(t_{m_j}) > U_g) && (b) \end{aligned}\right\}, \tag{7}$$

where: j is the cycle number of the UV light source; n_j and m_j are the high-impedance voltmeter sampling periods in the light off phase and the illumination phase in an ON-OFF control period; Δt is the sampling period of high-impedance voltmeter; $U_f^{-1}(U(t_{m_j}))$ is the inverse function of the driving voltage equation in the light off phase.

If the optical shutter is closed, and the driving voltage value of the high-impedance voltmeter in the next sampling period can be calculated by Eq. (8):

$$\left.\begin{aligned} U &= U_i + U_f^{-1}(U(t_{m_j}))\Delta t && (a) \\ t_{m_j} &= U^{-1}(U_f(t_{n_j})), \quad U_f(t_{n_j}) \le U_g && (b) \end{aligned}\right\}, \tag{8}$$

where: $U^{-1}(U_f(t_{n_j}))$ is the inverse function of the driving voltage equation for the illumination phase.

3. Comparing the current driving voltage U obtained in step (2) with the target voltage value U_g, when U is greater than U_g, the optical shutter is closed; when U is less than U_g, the optical shutter is opened.

4. The given cycle time is compared with the total system running time. When T is less than t, the cycle repeats step (1). When T is greater than t, the control ends.

4.2. Parameter identification

In the previous section, according to the closed-loop control mechanism and theoretical derivation, the closed-loop control model is given, and the driving voltage expressions in the light on and light off phases are obtained. In order to carry out the closed-loop control simulation verification, an open-loop measurement of the driving voltage is required.

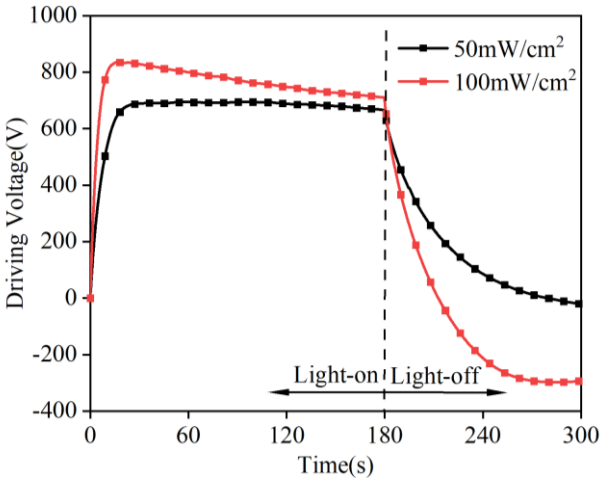

Fig. 8 Driving voltage curve when the necking width is 2 mm

In the experiment, the driving voltage value of the actuator when the necking width w_2 is 2mm is measured under the condition of the illumination intensities of 50 mW/cm^2 and 100 mW/cm^2 respectively, the measurement time is 300 s, and the illumination time is 180 s. The driving voltage curves of the photoelectric actuator is shown in Fig. 8.

As shown in Fig. 8, in the illumination phase of PLZT ceramic, the driving voltage reaches the saturation value under irradiation of 50 mW/cm^2 and remains in a stable state; while, under irradiation of 100 mW/cm^2, the driving voltage rapidly reaches the saturation value, then it drops to a certain stable state. In the light off phase, the driving voltage drops rapidly to a certain stable value.

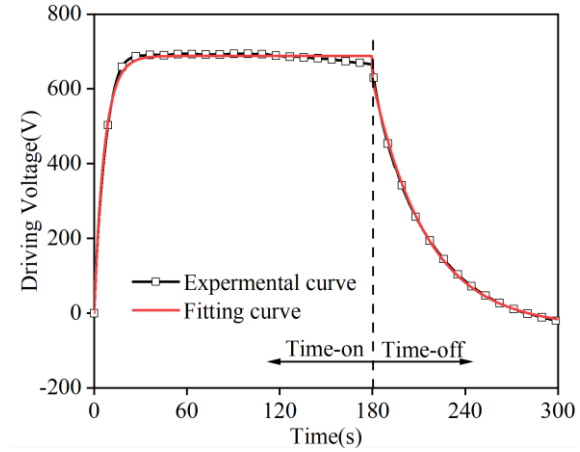

a

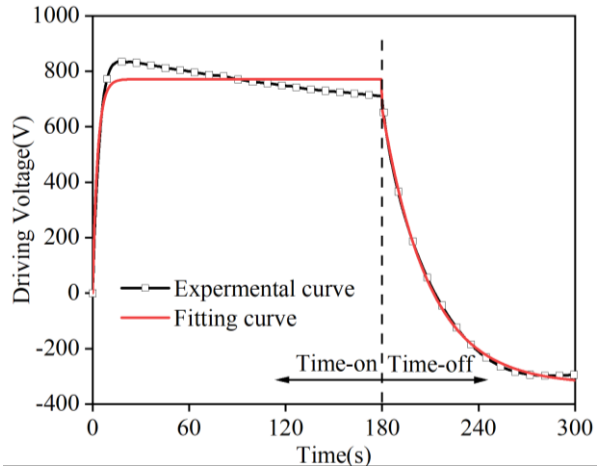

b

Fig. 9 Experimental and fitting curves of driving voltage under different light intensities: a) under irradiation of 50 mW/cm^2; b) under irradiation of 100 mW/cm^2

According to the mathematical model equation (6) of the driving voltage obtained in the previous section, the above experimental curves are fitted to obtain the driving voltage fitting curves, which can be shown in Fig. 9.

It is known from Fig. 9 that the fitting curve of the driving voltage is basically consistent with the experimental curves, and the fitting effect is well.

According to the fitting results, Tables 2 and 3 show the fitting values of the corresponding parameters in the mathematical model Eq. (6) can be achieved when the light intensities are 50 mW/cm^2 and 100 mW/cm^2.

Table 2

Fitting values of parameters of driving voltage expression in light-on phase

Light intensity, mW/cm^2	Driving voltage saturation value U_s', V	Driving voltage time constant τ', s
50	688.16	6.64
100	770.3	3.12

Table 3

Fitting value of parameters of driving voltage expression in light-off phase

Light intensity, mW/cm^2	The initial voltage U_0, V	Residual voltage variation coefficient k_f	Driving voltage time constant τ_f
50	-37.74	662.03	35.12
100	-329.75	995.63	28.94

According to Table 2 and Table 3, the driving voltage expressions of the light on and light off phases can be obtained when the light intensities are 50 mW/cm^2 and 100 mW/cm^2 respectively:

$$\left.\begin{aligned} U(t) &= 688.16(1-e^{-\frac{t}{6.64}}) \quad (t \le 180) \\ U_f(t) &= -37.74 + 662.03e^{-\frac{t}{35.12}} \quad (t > 180) \end{aligned}\right\}, \tag{9}$$

$$\left.\begin{aligned} U(t) &= 771.3(1-e^{-\frac{t}{3.12}}) \quad (t \le 180) \\ U_f(t) &= -329.75 + 995.63e^{-\frac{t}{28.94}} \quad (t > 180) \end{aligned}\right\}. \tag{10}$$

4.3. Simulation process and results

According to the closed-loop control model of the driving voltage, the closed-loop control simulation flow of the ON-OFF control strategy is developed in Fig. 10.

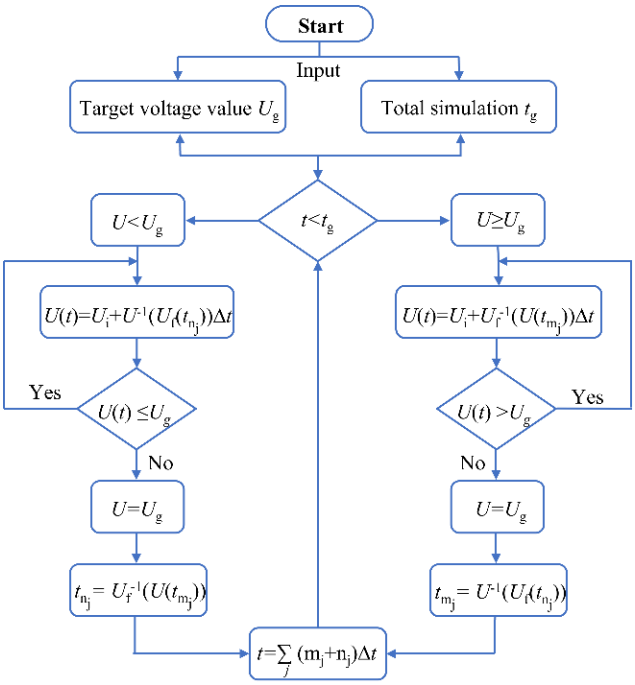

Fig. 10 The ON-OFF closed-loop control simulation flow

Before the simulation starts, the driving voltage target value U_g and the simulation time t_g are input to the computer first. When the simulation starts, the closed-loop control model is used to simulate the variation trends of the driving voltage in the illumination and the light-off phases respectively. When the driving voltage U is less than or equal to the target voltage U_g, the system calls the ON function written by the Eq. (7a), and calculates the initial condition of the opposite trend is calculated by the Eq. (7b); When the driving voltage U is greater than the target voltage U_g, the system calls the OFF function written by the Eq. (8a), and the initial condition of the opposite trend is calculated by the Eq. (8b). The optical shutter is continuously opened and closed cyclically, which causes the UV light to continuously switch between the illumination and the light-off phases. Therefore, the driving voltage will continuously fluctuate up and down the target value until the simulation time t reaches the set simulation total time t_g.

Using Eqs. (9) ~ (10), the driving voltage simulation of photoelectric actuator is carried out under the light intensities of 50 mW/cm^2 and 100 mW/cm^2. The target voltage U_g is set to 500 V, the simulation time is 120 s, and the sampling period Δt is 200 ms, as shown in Fig. 11.

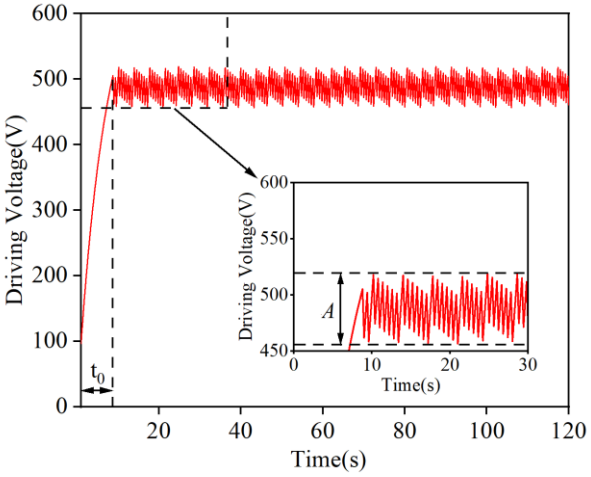

a

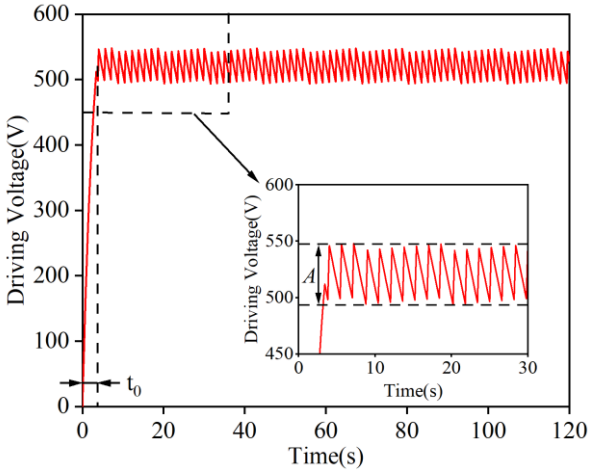

b

Fig. 11 Simulation curve of driving voltage when the target voltage is 500V: a) under irradiation of 50 mW/cm^2; b) under irradiation of 100 mW/cm^2

Fig. 11 shows that when PLZT ceramic is illuminated under 50 mW/cm^2 and 100 mW/cm^2, the driving voltages reach the target value U_g (500 V) within 8.61 s and 3.26 s respectively, and the ON-OFF control strategy is adopted to realize the closed-loop control of the driving voltage. The driving voltages fluctuate in the range of 54.4 V~62.58 V respectively, and the fluctuation rate is 1.3%~9.51%.

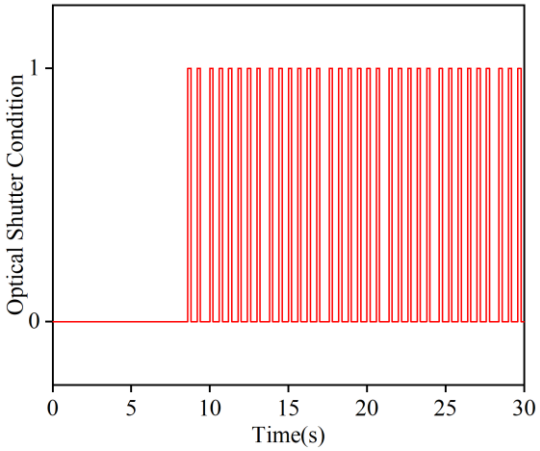

a

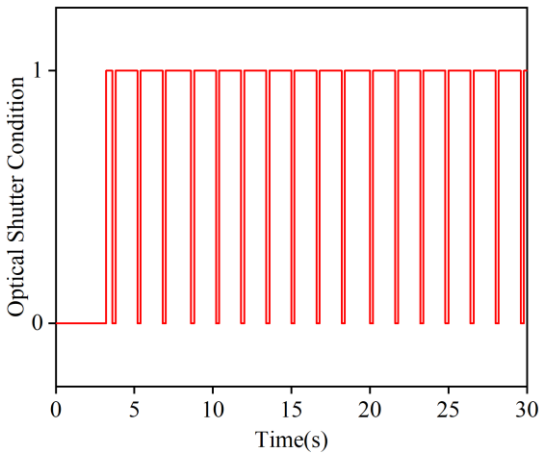

b

Fig. 12 Light shutter condition: a) under irradiation of 50 mW/cm^2; b) under irradiation of 100 mW/cm^2

At the same time, the state change of the optical shutter can be judged. If 0 represents open of the optical shutter, and the 1 represents close of the optical shutter, the state of the optical shutter within 30s after the light is turned on can be expressed by Fig. 12. From Fig. 12, by implementing the ON-OFF closed-loop control strategy, the state of the optical shutter is continuously cyclically switched between open and close so that the driving voltage can be controlled within the range of the amplitude A around the target value. To better verify the effectiveness of the ON-OFF closed-loop control, the simulation when the target voltage U_g is 600 V is carried out, as shown in Fig. 13.

It can be observed from Fig. 13 that when the target value U_g is set to 600 V, the driving voltages reach the target value within 13.64 s and 4.7 s respectively under the illumination of 50 mW/cm^2 and 10 0mW/cm^2. Through the ON-OFF closed-loop control strategy, the driving voltage can still be effectively controlled. The driving voltages fluctuate in the range of 54.08 V~62.58 V respectively, and the fluc-

tuation rate is 1.07%~7.94%. According to the above control simulation results with different target values, the proposed ON-OFF closed-loop control strategy has perfect feasibility, and its effectiveness in multi-objective closed-loop control is proved.

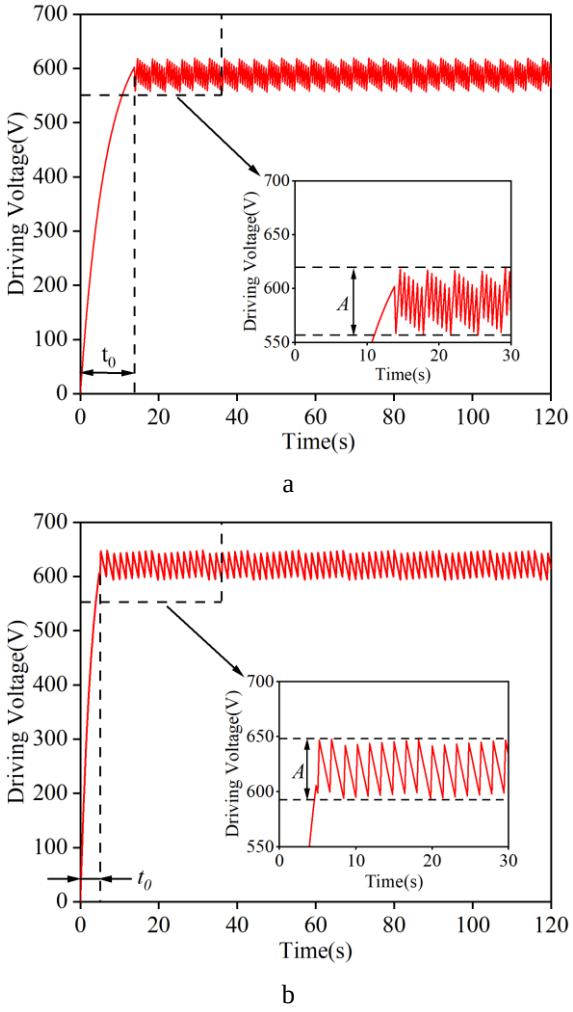

Fig. 13 Simulation curve of driving voltage when the target voltage is 600 V: a) under irradiation of 50 mW/cm^2; b) under irradiation of 100mW/cm^2

5. Closed-loop control of output displacement

Similarly, the closed-loop control of the output displacement as the control variable is similar in principle and simulation process to the closed-loop control of the driving voltage as the control variable in the previous section.

Based on the control model, according to Eq. (1) and Eqs. (9) ~ (10), the output displacements of the actuator in the light on and the light off phases can be obtained when the light intensities are 50 mW/cm^2 and 100 mW/cm^2 and the width of the necking structure is 2 mm:

$$\left.\begin{aligned} S(t) &= 37.16(1-e^{-\frac{t}{6.64}}) \\ S_f(t) &= -2.04+35.75e^{-\frac{t}{35.12}} \end{aligned}\right\}, \tag{11}$$

$$\left.\begin{aligned} S(t) &= 41.65(1-e^{-\frac{t}{3.12}}) \\ S_f(t) &= -17.81+53.76e^{-\frac{t}{28.94}} \end{aligned}\right\}. \tag{12}$$

Using the Eqs. (11) ~ (12), the output displacement simulation of photoelectric actuator is carried out under the irradiation of 50 mW/cm^2 and 10 0mW/cm^2. The target displacement S_g is set to 25 μm, the simulation time is 120 s, and the sampling period Δt is 200 ms, as shown in Fig. 14.

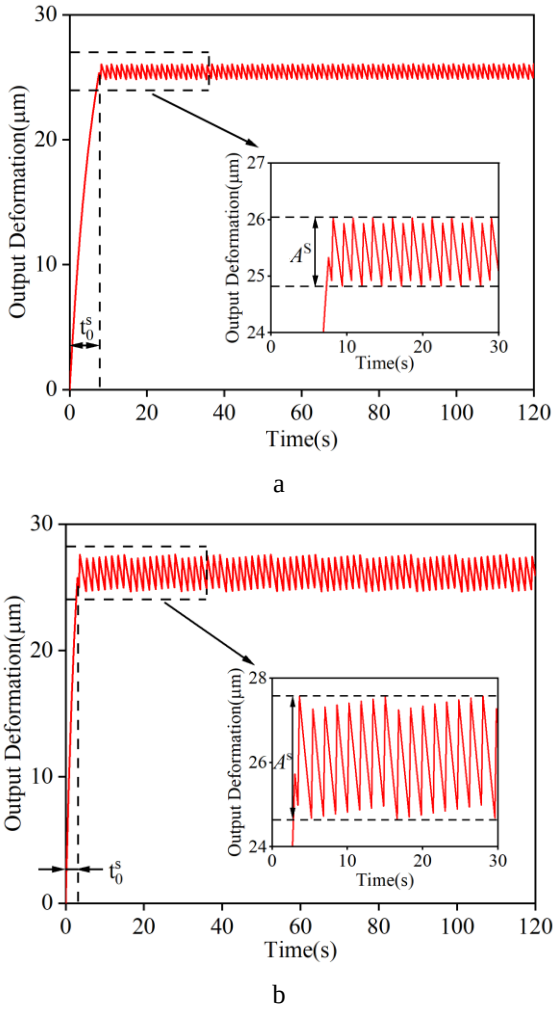

Fig. 14 The output displacement simulation curve when the target displacement is 25 μm: a) under irradiation of 50mW/cm^2; b) under irradiation of 100 mW/cm^2

From Fig. 14, under the illumination of 50 mW/cm^2 and 100 mW/cm^2, the output displacements reach the target value S_g (25μm) within 7.42 s and 2.86 s respectively, the ON-OFF control strategy is adopted to realize the closed-loop control of output displacement. The output displacements fluctuate in the range of 1.23 μm ~ 2.93 μm respectively, and the fluctuation rate is 0.68%~10.28%. At the same time, the simulation is carried out under the condition that the target displacement value S_g is 30 μm to better verify the effectiveness of the closed-loop control, as shown in Fig. 15.

It can be observed from Fig. 15 that when the output displacement target value S is set to 30 μm, the output displacements reach the target value within 10.93 s and 3.98 s respectively under irradiation of 50 mW/cm^2 and 100mW/cm^2, the output displacement can still be effectively controlled by the ON-OFF closed-loop control strategy. The driving voltages fluctuate in the range of 1.23 μm ~ 2.93 μm respectively, and the fluctuation rate is 0.52%~8.56%. According to the analysis of the above control results using the

driving voltage and output displacement as the control variables, the proposed closed-loop control method under the ON-OFF control strategy has good control performance. At the same time, its feasibility and effectiveness are also verified.

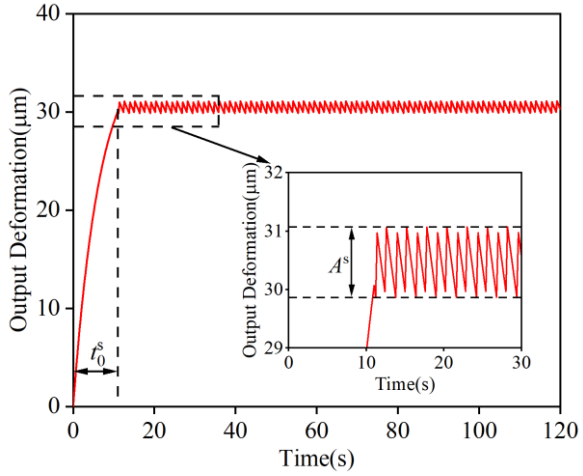

a

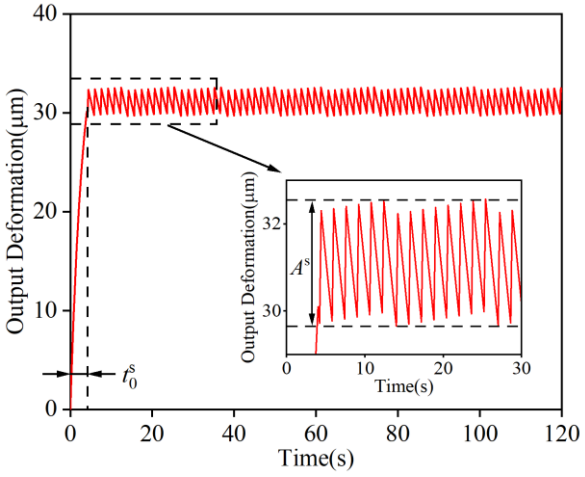

b

Fig. 15 The output displacement simulation curve when the target displacement is 30 μm: a) under irradiation of 50 mW/cm^2; b) under irradiation of 100 mW/cm^2

6. Conclusion

Aiming at the low control precision of micro actuators, a new ON-OFF closed-loop control method of photoelectric actuator based on PLZT ceramic is proposed in this paper. Firstly, on the basis of the theoretical model of ON-OFF control strategy, the closed-loop control analysis and model parameter identification are carried out with driving voltage and output displacement as control variables. Then the model under multi-voltage and multi-light intensity is simulated and analyzed. The results show that when the target voltages are 500 V and 600 V, the driving voltage reaches the target value within 3.26 s~13.64 s, respectively, and the voltage fluctuation rate is 1.07%~9.51%. When the target displacements are 25 μm and 30 μm, the output displacement reaches the target value within 2.86 s~10.93 s, respectively, and the displacement fluctuation rate is 0.52%~10.28%. According to the control effect, the feasibility and effectiveness of the actuator control strategy are verified, which provides a new idea for improving the control accuracy of micro actuators, and promotes the application of photoelectric actuators based on PLZT ceramic in the field of active control.

Acknowledgments

This work is supported by the National Natural Science Foundation of China (No. 52075263), the Supported by the Innovative Funds Plan of Henan University of Technology (No. 2020ZKCJ28), the Foundation of the Education Department of Henan Province (No. 23A460002) and the Foundation of Henan University of Technology (No. 31401426).

References

1. **Liu, Y.; Wang, X; Wang, J; Chen, H.; Huang, J.** 2020. The experimental analysis on the driving characteristics of photo response torsion actuator, Journal of Intelligent Material Systems and Structures 31(12): 1455-1464. https://doi.org/10.1177/1045389X20923092.
2. **Yue, H.; Jiang, J; Long, Y; Song, Y.** 2014. Modelling and experiments of PLZT/PVDF hybrid drive method for non-contact shape adjustment, International Journal of Applied Electromagnetics and Mechanics 46(4): 867-877. https://doi.org/10.3233/JAE-140095.
3. **Chen, X.; Chen, R.; Chen, Z.; Chen, J.; Shung, K.; Zhou, Q.** 2016. Transparent lead lanthanum zirconate titanate (PLZT) ceramic fibers for high-frequency ultrasonic transducer applications, Ceramics International 42(16): 18554-18559. http://dx.doi.org/10.1016/j.ceramint.2016.08.195.
4. **Rahman, M.; Ahmed, M.; Nawaz, M.; Molina, G.; Rahman, A.** 2017. Experimental investigation of photostrictive materials for MEMS application, Open Access Library Journal 4(11): 1. https://doi.org/10.4236/oalib.1103856.
5. **Wang, L.; Zheng, S.** 2018. Nonlinear analysis of 0–3 polarized PLZT microplate based on the new modified couple stress theory, Physica E: Low-dimensional Systems and Nanostructures 96: 94-101. https://doi.org/10.1016/j.physe.2017.10.001.
6. **Chen, M.; Zheng, S.** 2019. Size-dependent models of 0–1/0–3 polarized PLZT unimorphs and bimorphs based on a modified couple stress theory, Mechanics Research Communications 98: 42-49. https://doi.org/10.1016/j.mchrescom.2018.08.015.
7. **Velosa, L.; Aguilera, L.; González, M.; Raskin, J.; Herrera, A.** 2018. Design of a novel MEMS microgripper with rotatory electrostatic comb-drive actuators for biomedical applications, Sensors 18(5): 1664. https://doi.org/10.3390/s18051664.
8. **Batra, V.; Kotru, S.** 2018. A simulation model for understanding the charge transport and recombination behavior in PLZT based ferroelectric photovoltaic devices, Ferroelectrics 532(1): 121-137. https://doi.org/10.1080/00150193.2018.1430433.
9. **Jiang, J.; Lu, Y.; Yan, X.; Wang, L.** 2020. An optimization dust-removing electrode design method aiming at improving dust mitigation efficiency in lunar exploration, Acta Astronautica 166: 59-68.

https://doi.org/10.1016/j.actaastro.2019.10.004.
10. **Jiang, C.; Huang, J.** 2021. Optimal design of a light operated micromanipula-tion based on opto-electrostatic repulsive actuator, 2020 15th Symposium on Piezoelectrcity, Acoustic Waves and Device Applications (SPAWDA), IEEE, p. 329-333. https://doi.org/10.1109/SPAWDA51471.2021.9445425
11. **Irschik, H.; Krommer, M.; Pichler, U.** 2003. Dynamic shape control of beam-type structures by piezoelectric actuation and sensing, International Journal of Applied Electromagnetics and Mechanics 17(1-3): 251-258. https://doi.org/10.3233/JAE-2003-251.
12. **Shih, H.; Tzou, H.; Saypuri, M.** 2005. Structural vibration control using spatially configured opto-electromechanical actuators, Journal of Sound and Vibration 284(1-2): 361-378. https://doi.org/10.1016/j.jsv.2004.06.013.
13. **Mahmoudpour, M.; Zabihollah, A.; Vesaghi, M.; Kolbadinejad, M.** 2014. Design and analysis of an innovative light tracking device based on opto-thermo-electro-mechanical actuators, Microelectronic engineering 119: 37-43. http://dx.doi.org/10.1016/j.mee.2014.01.019.
14. **Lu, F.; Wang, X.; Huang, J.; Liu, Y.** 2016. Theoretical and experimental analysis of an optical driven servo system, Smart Materials and Structures 25(9): 095054. https://doi.org/10.1088/0964-1726/25/9/095054.
15. **He, R.; Zheng, S.; Tong, L.** 2016. Multimodal vibration control of photo-electric laminated thin cylindrical shells via self-organizing fuzzy sliding mode control, Journal of Vibration and Acoustics 138(4). https://doi.org/10.1115/1.4033195.
16. **Jiang, J.; Li, X.; Ding, J.; Yue, H.; Deng, Z.**2016. Mathematical model and characteristic analysis of hybrid photovoltaic/piezoelectric actuation mechanism. Smart Materials and Structures, 25(12): 125021. https://doi.org/10.1088/0964-1726/25/12/125021.
17. **Gou, X.; Liu, B.** 2018. Study on vibration control of simply supported plate based on fuzzy neural network, Computer and Digital Engineering 46(8): 1564-1567. https://doi.org/ 10. 3969/j. issn. 1672-9722.
18. **Bakhtiari, I.; Behrouz, S.; Rahmani, O.** 2020. Nonlinear forced vibration of a curved micro beam with a surface-mounted light-driven actuator, Communications in Nonlinear Science and Numerical Simulation 91: 105420. https://doi.org/10.1016/j.cnsns.2020.105420.
19. **Huang, W.; Lian, J.; An, D.; Chen, M.; Lei, L.** 2022. Bidirectional drive with inhibited hysteresis for piezoelectric actuators, Sensors 22(4): 1546. https://doi.org/10.3390/s22041546.
20. **Liu, Y.; Wang, X.; Wang, J.; Chen, H. Huang, J.** 2021. Investigation on influence factors of opto-electrostatic hybrid driving torsion actuator based on PLZT ceramic, Materials Science and Engineering: B 263: 114798. https://doi.org/10.1016/j.mseb.2020.114798.

Y. Liu, Y. Yang, C. Liu, X. Wang

AN ON-OFF CLOSED-LOOP CONTROL OF PHOTOELECTRIC ACTUATOR BASED ON PLZT CERAMIC

S u m m a r y

PLZT (lanthanum-doped lead zirconate titanate) ceramic with outstanding photostrictive effect has been widely used in the micro precision drive field. In this article, a new closed-loop control method with ON-OFF control strategy is proposed for the photoelectric actuator based on PLZT ceramic. The closed-loop control model under driving voltage control strategy is established, and the parameters are identified by a series of experiments. Then, the control equations of driving voltage and output displacement of the photoelectric actuator are derived on the basis of the closed-loop control model during the light on and light off phases. After that, the numerical simulation analysis is carried out when the driving voltage and output displacement are taken as control objects respectively. According to the analysis results, the output displacement of the photoelectric actuator can be successfully controlled at a specific target value, and the proposed control method has excellent control effect, the feasibility and effectiveness of the control method are verified. Relevant conclusions can lay a foundation and provide theoretical guidance for the practical application of the photoelectric actuator in the field of active control.

Keywords： PLZT ceramic, photostrictive effect, photoelectric actuator, closed-loop, ON-OFF control

Received March 26, 2023
Accepted December 3, 2023